Convective Structure of Hurricanes as Revealed by Lightning Locations

JOHN MOLINARI, PAUL MOORE, AND VINCENT IDONE

Department of Earth and Atmospheric Sciences, The University at Albany, State University of New York, Albany, New York

(Manuscript received 27 August 1997, in final form 26 February 1998)

ABSTRACT

Cloud-to-ground lightning flash locations were examined for nine Atlantic basin hurricanes using data from the National Lightning Detection Network. A common radial distribution in ground flash density was evident: a weak maximum in the eyewall region, a clear minimum 80–100 km outside the eyewall, and a strong maximum in the vicinity of outer rainbands (210–290-km radius). These results are consistent with the authors' previous study of Hurricane Andrew. None of the storms showed this characteristic radial structure during prehurricane stages.

The results support the division of precipitation in the hurricane into three distinct regimes. The eyewall is a unique phenomenon but shares some attributes with deep, weakly electrified oceanic monsoonal convection. The region outside the eyewall and under the central dense overcast has characteristics of the trailing stratiform region of mesoscale convective systems, including a relatively high fraction of positive polarity flashes. The outer bands, with mean maximum flash density at the 250-km radius, contain the vast majority of ground flashes in the storms.

Eyewall lightning, defined as that within 40 km of the center, was examined for four moderate-to-strong hurricanes. Such lightning occurred episodically during hurricane stage, with 93% of hourly intervals containing *no* detected flashes. Eyewall lightning outbreaks over water always occurred at the beginning of or during times of intensification, but often were indicative of the imminent end of deepening. It is proposed that the existence of such inner core lightning might reveal the presence of an eyewall cycle. For the one storm with available aircraft reconnaissance data, eyewall cycles were reliably identified by the occurrence of inner core lightning, and inner core lightning appeared only during such cycles. Suggestions are made as to how eyewall flashes in existing hurricanes might be used to help predict hurricane intensity change.

1. Introduction

Molinari et al. (1994) and Samsury and Orville (1994) showed that the National Lightning Detection Network (NLDN) could profitably be used to study lightning in hurricanes, even while the storms were outside the network over water. Molinari et al. (1994) examined the temporal and spatial variation of lightning for a 64-h period during Hurricane Andrew (1992). Samsury and Orville (1994) examined the distribution of lightning in Hurricanes Hugo and Jerry of 1989 as they made landfall. In addition, Lyons and Keen (1994), using Lightning Position and Tracking System (LPATS) data, described lightning in four tropical storms in the Gulf of Mexico. Williams (1995) and Lascody (1992) also used LPATS to examine lightning in Hurricane Andrew just before it made landfall in Florida.

Molinari et al. (1994) divided the hurricane into three regions based on electrical characteristics: eyewall; inner bands, extending 20–80 km outside the eyewall; and outer bands, beginning outside of the 100-km radius and reaching peak flash density at the 190-km radius. Molinari et al. (1994) made the following conclusions concerning lightning observed in Hurricane Andrew: (i) eyewall cloud-to-ground lightning outbreaks occurred episodically; (ii) such outbreaks occurred only during or just before intensification of the hurricane; (iii) all intensification periods contained such outbreaks; (iv) evidence supported the existence of an outwardly sloping dipole in the eyewall, with positive flashes occurring radially outward from negative flashes; (v) ground flash density was sharply suppressed from outside the eyewall to the 100-km radius; (vi) the vast majority of ground flashes occurred in outer rainbands well outside of the radius of hurricane force winds; and (vii) an average of 4400 flashes per day occurred within 300 km of the hurricane center.

Samsury and Orville (1994) described two storms whose behavior was quite different than Hurricane Andrew. Intense Hurricane Hugo had only 33 flashes in 18 h, and marginal Hurricane Jerry had only 691 in 18 h. Most of the ground flashes in Hurricane Jerry occurred in rainbands 50–75 km outside the storm center before landfall, and in or near the eyewall after landfall. Both hurricanes had a percentage of positive ground flashes

Corresponding author address: Dr. John Molinari, Department of Earth and Atmospheric Science, SUNY—Albany, Albany, NY 12222. E-mail: molinari@atmos.albany.edu

that was much higher than the network average. Few flashes occurred more than 100 km from the center of either storm.

Lyons and Keen (1994) described lightning variation in an unnamed tropical storm, mostly over land, in 1987, and in Hurricanes Diane (1984), Florence (1988), and briefly in Hurricane Elena (1985). Their sensors predominantly detected cloud-to-ground lightning, plus the most intense intracloud strokes. Both Hurricanes Diane and Florence showed significant outbreaks of lightning near the center before or during intensification. Although the radial distribution of flashes was not shown, overall ground flash frequency appeared to be greatest in the outer bands ($r > 200$ km) of Hurricane Diane. Flash frequency was high close to the center in Hurricane Florence, particularly as it intensified.

Williams (1995) and Lascody (1992) found that Hurricane Andrew (1992) had an outbreak of lightning around the eyewall as it rapidly deepened just before its Florida landfall. The timing and distribution of the flashes were quite similar to those derived from the NLDN (Molinari et al. 1994).

Overall, the above studies showed considerable variation among hurricanes in overall ground flash frequency and its radial distribution. Some promising results on the predictive value of ground flashes in the core of hurricanes were shown. This study is designed to extend the previous results to nine Atlantic hurricanes, four of which were also studied by Samsury and Orville (1994) or Lyons and Keen (1994). Based on the distribution of cloud-to-ground lightning and the results of previous studies, some inferences will be made about the convective structure of hurricanes.

2. Data sources

a. Lightning data

Data were obtained from archived observations of the NLDN (Orville 1991). For the times of storms in this study (1985–91), the NLDN consisted of up to 100 magnetic direction-finding sensors (DFs) that covered the continental United States (Cummins et al. 1992). The current configuration of the network, which now contains a mix of sensor types, is described by Cummins et al. (1998). Though originally developed at the University at Albany, the NLDN is presently operated and maintained by Global Atmospherics, Inc., of Tucson, Arizona.

As is true of all remote sensing systems, possible errors in the data and inherent limits of the system must be accounted for when interpreting the results. These factors were discussed in detail by Cummins et al. (1992) and, for hurricane studies, by Molinari et al. (1994). The current work includes four storms prior to 1987, during the early years of the NLDN. Statistical site corrections during those years had to be determined from relatively small datasets [site corrections are required to compensate for systematic errors at certain azimuth angles caused by local topographical variations or reradiation sources peculiar to a given site (see Horner 1954; Knight 1967; Hiscox et al. 1984)]. Flash locations and characteristics were recalculated for Hurricane Bob (1985) using recent, more accurate site corrections. Both the initial and the recalculated ground flash locations were overlaid on satellite images. Each dataset contained excellent agreement in general between lightning locations and the location of deep clouds on satellite. In the original data, however, a small area south of the Florida panhandle contained systematic shifts of the lightning as much as 50 km away from its associated convective clouds on satellite images. The revised site corrections virtually eliminated this error. As a result, lightning data from all storms were reprocessed using the revised site corrections.

A number of characteristics of the NLDN are relevant to the current study: (i) nominal observation range of the network, (ii) location error, (iii) detection efficiency less than 100%, and (iv) variation in the last two characteristics with distance from the network.

Each DF can sense flash polarity accurately to about 600 km, but location errors increase with range. In the current study, tropical cyclones were included in the dataset only when their center passed within 400 km of at least one DF. Because a storm just inside the edge of this region will have almost half its circulation outside the nominal range, azimuthal variation of flash density must be interpreted with caution.

Location accuracy is important for this study, because the radial distribution of flash density in 20-km bins is of primary interest. Idealized models suggest that the median location error is 3 km within the network and increases to about 8 km at a distance of 400 km from the edge of the network (Cummins et al. 1992). Estimates of actual median errors have ranged from 2 to 4 km (Holle and Lopez 1993) to 8 km (Maier 1991). Lightning field studies using a network of video cameras deployed in the Albany, New York, area during the summers of 1994–95 (Idone et al. 1998a,b) found a median location accuracy of better than 3.5 km for the configuration relevant to the observation times in this study. Relevant to future studies of tropical cyclones, the new configuration of the network appears to have a fivefold increase in location accuracy (Idone et al. 1998b).

No formal study has been done of NLDN accuracy over water, but Molinari et al. (1994, their Fig. 6) and Samsury and Orville (1994, their Figs. 4 and 6) show some encouraging results. In each study, NLDN-derived ground flash locations corresponded closely with radar reflectivity maxima during periods that Hurricanes Andrew, Hugo, and Jerry were off the coasts of Florida, South Carolina, and Louisiana, respectively. In addition, plate 1 from Molinari et al. (1994) shows that when large numbers of flashes occurred, they represented a coherent feature even if individual flashes might not have been perfectly positioned. Rainbands over the Gulf

TABLE 1. List of storms and the hours they were within range of the NLDN. ''Intensity'' gives the average maximum wind speed ($m\ s^{-1}$) over the period of interest. ''Pre'' indicates the period prior to hurricane intensity.

Storm	Intensity ($m\ s^{-1}$)	Begin/end	Hours	Number of flashes
Pre-Bob (1985)	20	00 UTC 22 Jul 16 UTC 24 Jul	65	10 522
Bob (1985)	32	17 UTC 24 Jul 04 UTC 25 Jul	12	2 841
Elena (1985)	47	11 UTC 30 Aug 12 UTC 2 Sep	74	1 758
Gloria (1985)	41	16 UTC 26 Sep 00 UTC 28 Sep	33	7
Pre-Charley (1986)	24	18 UTC 15 Aug 09 UTC 17 Aug	40	4 682
Charley (1986)	34	10 UTC 17 Aug 09 UTC 18 Aug	24	4 031
Florence (1988)	34	18 UTC 09 Aug 05 UTC 10 Aug	12	197
Chantal (1989)	35	22 UTC 31 Jul 14 UTC 1 Aug	17	1 525
Hugo (1989)	56	18 UTC 21 Sep 09 UTC 22 Sep	16	35
Jerry (1989)	35	16 UTC 15 Oct 03 UTC 16 Oct	12	336
Pre-Bob (1991)	24	00 UTC 17 Aug 17 UTC 17 Aug	18	1 637
Bob (1991)	42	18 UTC 17 Aug 22 UTC 19 Aug	53	3 279

of Mexico could be easily tracked in time using lightning locations alone.

In the Hurricane Andrew study (Molinari et al. 1994) each flash was overlaid on hourly infrared satellite images. With the exception of a small region north of Cuba, flashes virtually always were coincident with convective clouds. In the small erroneous region, baseline effects (a narrow angle between azimuth vectors of two DFs) appeared to be responsible. Other than this narrow region, the previous study suggests that the vast majority of flashes were well located with respect to the satellite-image measure of ground truth. With the updated site corrections described above, we expect the flash locations in the current study to be equally satisfactory.

Detection efficiency within the network over land typically varies from 50% to 80%, with stronger flashes (greater than 14-kA peak current) detected nearly 100% of the time (see, e.g., Idone et al. 1998a). Outside the network it would likely be lower, and it is clear that only a portion of the ground flashes that occur over water will be sampled. It is the relative frequency rather than the absolute number of ground flashes in various parts of the hurricane that is of interest. Absolute flash counts will be compared between storms, but these vary over a range of three orders of magnitude, far more than the possible error in such counts.

Because detection efficiency decreases with increasing distance from the network, caution must be used in interpreting the time variation of flashes as a storm approaches the coast. Nevertheless, it will be shown in this study that both the temporal and spatial variations of flash frequency show no apparent relationship with the distance of a storm from the network. As long as data collection is restricted to times of the storm center within 400 km of a DF, the physical mechanisms that control lightning frequency in the hurricane apparently have a much larger influence than the distance-dependent sensitivity of the NLDN. Although limitations of the lightning data must not be ignored, the evidence from the studies of Molinari et al. (1994) and Samsury and Orville (1994) strongly suggests that useful analyses can be carried out with the available data.

b. Hurricane data

Positions and intensity of hurricanes at 6-hourly intervals were obtained from the ''best-track'' data produced by the National Hurricane Center. Table 1 lists the nine tropical cyclones studied in this paper and the times their centers were in range of the NLDN (i.e., within 400 km of at least one DF) during both hurricane and prehurricane stages. Five marginal hurricanes (32–35 $m\ s^{-1}$ mean maximum sustained surface wind speed during the period the storm was within range of the

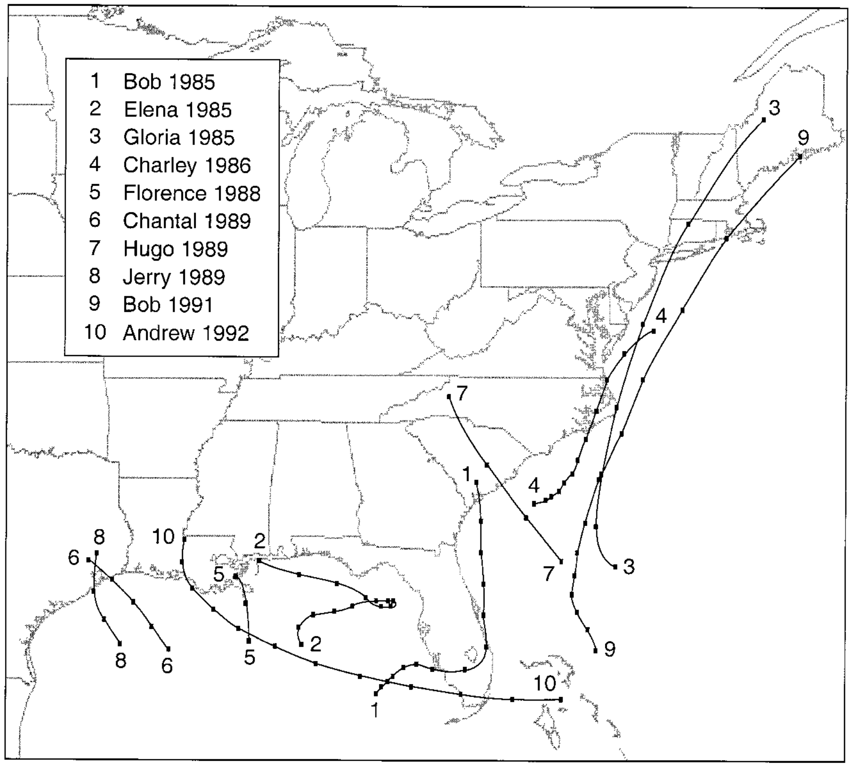

FIG. 1. Six-hourly positions of the nine hurricanes examined in this paper during the periods they were within 400 km of at least one DF. The track of Hurricane Andrew (1992), studied by Molinari et al. (1994), is included for comparison.

NLDN), three moderate hurricanes (41–47 m s^{-1}), and one strong hurricane (56 m s^{-1}) were observed. The previous storm studied, Hurricane Andrew, had a mean maximum wind speed of 60 m s^{-1} and ranked with Hurricane Hugo as a strong storm. With the exception of Hurricane Gloria, each storm was within range of the NLDN at or just after its time of maximum intensity. Analyses were extended after landfall as long as hurricane strength was maintained.

Minimum central pressure was also taken from the best-track values every 6 h. Occasionally large pressure changes are observed by reconnaissance aircraft on a smaller timescale than the best-track data. Such was the case for Hurricane Andrew prior to landfall (Molinari et al. 1994) and for Hurricane Elena in this study. For those storms, a 3-hourly dataset was constructed using a combination of best-track and reconnaissance data. In addition, the best-track pressure was supplemented for Hurricane Hugo with the minimum pressure at landfall, which occurred in between best-track times. Other storms in this study contain 6-hourly pressure only. It is possible, of course, that rapid pressure fluctuations on small timescales are being missed. The comparison of central pressure changes and flash count is only meaningful over a 3- or 6-h average.

Figure 1 shows the track of each storm at 6-hourly increments during the periods for which lightning data were examined. All storms between 1985 and 1991 that moved within 400 km of at least one DF while at hurricane intensity were included in this study. Data were also collected for the three storms that were within range of the network during their prehurricane stages. Because the NLDN has grown dramatically with time and now covers the continental United States (Orville 1991), early storms are less likely to be within 400 km of one DF than later storms. In particular, several hurricanes in the western Gulf of Mexico could not be observed in 1985, and Hurricane Elena of 1985 could not be observed after landfall. Nevertheless, a total of 376 h of lightning data were collected from the nine storms, 253 at hurricane intensity, and 123 during prehurricane stages.

3. Interpretation of cloud-to-ground lightning data

Rutledge et al. (1990); Rutledge et al. (1992), Williams et al. (1992), and Zipser and Lutz (1994) have provided insightful discussions of how to interpret lightning data in terms of vertical velocity, vertical profiles of radar reflectivity, and electrification mechanisms. Randell et al. (1994) have provided further insight via numerical simulations. Molinari et al. (1994) reviewed observational studies of hurricane convection, and Black et al. (1996) provided a comprehensive summary of Doppler-derived reflectivity and vertical velocity in hurricanes. Those aspects relevant to the current work will be briefly summarized in this section. Because no microphysical data are available for this study, many details of microphysics and electrification mechanisms will be omitted. These have been described in hurricanes by Black and Hallett (1986; 1997), Black et al. (1993), Williams (1995), and Houze et al. (1992). Saunders (1993) and the papers referenced earlier in the paragraph provide more general discussions of microphysics and charging mechanisms.

Three broad categories of convection have been differentiated on the basis of lightning data.

1) High-aspect-ratio deep convection with strong localized updrafts and downdrafts and a reflectivity maximum of 30–50 db*Z* above the melting level (Williams et al. 1992). In the DUNDEE experiment in Australia, these were primarily continental clouds that occurred during ''monsoon break periods'' in which low cloud amount is minimized [see Krishnamurti and Bhalme (1976) for a description of the radiative and convective characteristics of active and break periods of monsoons]. This type of convection is indicated in the lightning data by the presence of frequent flashes bringing negative charge to ground (''negative flashes''). The high flash rate is attributed to charge separation due to the simultaneous presence above the melting level of liquid water, large graupel, and ice (see review by Saunders 1993) as a result of strong local updrafts.
2) Convection with vertical velocities generally below 7 m s^{-1} averaged over 2–3 km, with 10–12 m s^{-1} peak updraft speed (Zipser and Lutz 1994), maximum reflectivity below the melting level (Rutledge et al. 1992), and a rapid decrease of radar reflectivity with height above the melting level (Szoke et al. 1986; Zipser and Lutz 1994). In contrast to 1), this type of convection contains a relatively low frequency of negative cloud-to-ground lightning around the convective core. The low negative flash rate is attributed to the weak vertical velocities that cannot maintain the necessary graupel particles in the mixed-phase region above the melting level.
3) Stratiform precipitation adjacent to active (or previously active) convection. This is marked by a higher percentage of flashes bringing positive charge to ground (''positive flashes'') than either of the above. A bright band exists on radar as frozen particles ejected from the convective updrafts grow by accretion, fall, and melt [see discussion by Yuter and Houze (1995)]. The positive flashes are attributed to one of two mechanisms: advection of positive charge away from the negative flash region in vertically sheared flow, which potentially exposes a positive charge center to ground (Brook et al. 1982; Rutledge and MacGorman 1988; Orville et al. 1988; Engholm et al. 1990); or in situ charging mechanisms in stratiform rain above the melting level (Rutledge et al. 1990; Rutledge and Petersen 1994; Engholm et al. 1990); or both mechanisms acting simultaneously at different levels (Stoltzenburg et al. 1994). An elevated fraction of positive flashes can also occur with localized supercell convection (Seimon 1993; MacGorman and Burgess 1994). No such events were observed within 300 km of any of the storms examined in this study.

The above distinctions suggest that cloud-to-ground lightning data provides additional information beyond that available from radar and from visible and infrared satellite images. For instance, the maximum radar reflectivity in hurricanes often occurs in the heavy rain falling out of the sloping eyewall (Marks and Houze 1987), not where updrafts are strongest. Infrared satellite images show broad regions of cold cloud top, but only a small fraction of such regions contain active convective updrafts (Yuter and Houze 1998). The presence of outbreaks of cloud-to-ground lightning should provide more precise locations of strong updrafts. In addition, the presence of an elevated percentage of positive flashes collocated with a minimum in total ground flashes would indicate a high likelihood of an anvil-type stratiform region. Finally, lightning can be sensed by the NLDN continuously over much of the storm circulation for many hours and for several hundred kilometers out to sea. Using this information it is hoped that the radial organization of the structure of convection within hurricanes can be investigated.

One limitation of the NLDN data used here is that no information exists on the frequency of intracloud flashes. It is possible that electrification could be occurring in the absence of cloud-to-ground flashes, and total flash rate would likely be of greater value than ground flashes alone. In this paper it will be assumed that the ratio of intracloud to ground flashes in hurricanes does not vary dramatically in time or space. This can be verified only by additional hurricane datasets that contain both types of flashes. In subtropical convection, Rutledge et al. (1992) found that the ratio of intracloud to ground flashes varied as the square root of the flash rate, from 2 to 5 at the low flash rates characteristic of most hurricane lightning. Although the range is large, it appears that intracloud flashes almost always accompany ground flashes. The occurrence of cloud-to-ground lightning is assumed to indicate at least moderate electrification. The absence of ground flashes for several hours or more will be interpreted as an indication of nonelectrified or weakly electrified clouds.

4. Lightning distribution in hurricanes

a. Storm-to-storm variability

Figure 2 shows the average daily flash rate within 300 km of the center for each storm, both prior (if available) and subsequent to the time of hurricane intensity. Hurricane Andrew (from Molinari et al. 1994) is in-

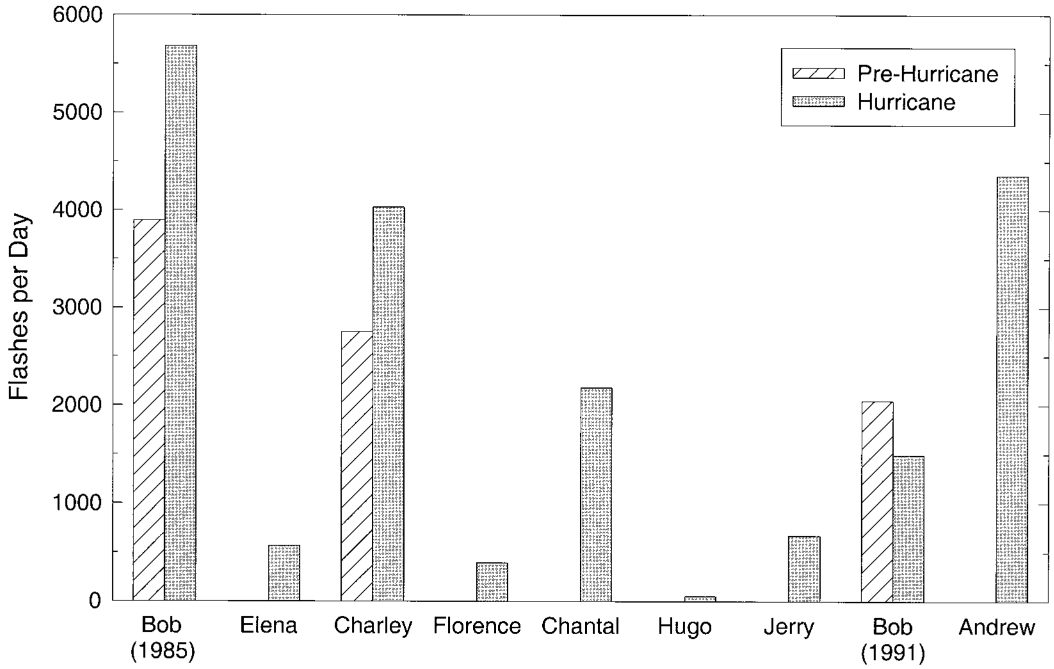

FIG. 2. Daily cloud-to-ground flash frequency within 300 km of the center for the 10 tropical cyclones indicated, during prehurricane stage (hatched) and hurricane stage (dark shading). The storms are arranged chronologically. Hurricane Gloria, with only seven flashes in 33 h, all after landfall, is not shown.

cluded for comparison. The average flash rate varied enormously from storm to storm, from near zero to more than 5700 per day. The two most intense storms contained both very low lightning frequency (Hurricane Hugo) and the second highest frequency (Hurricane Andrew), whereas the highest frequency occurred in marginal Hurricane Bob (1985). Moderate Hurricane Gloria (1985) had virtually no lightning and is not shown on the figure. It is apparent from Fig. 2 and Table 1 that no systematic relationship occurred between average intensity and average flash frequency over 300 km of radius.

Two storms containing both prehurricane and hurricane flash data (see Fig. 2) showed an increase in lightning frequency over 300 km of radius during hurricane stage, whereas one showed a decrease. Variations in lightning frequency from pre-hurricane to hurricane stage of a given storm were smaller than the storm-to-storm variability.

b. Radial distribution

Figures 3a,b show the distribution of flash density with radius, in 20-km annular rings, during the hurricane stage only of each storm, in units of flashes per 100 km $\times$ 100 km area per day. The storms are divided into two groups: those with maximum flash density exceeding 250 (100 km)$^{-2}$ day^{-1}, and those with maximum flash density less than 150 (100 km)$^{-2}$ day^{-1}. The radial distributions generally show three common features. The first is a maximum in ground flash density occurring in one of the inner three 20-km bins. Only Hurricane Charley (1986) failed to have this inner core maximum, and this storm was somewhat exceptional in that it was classified as ''subtropical'' by the National Hurricane Center, indicating that it lacked normal tropical cyclone characteristics, during much of its life cycle.

All inner core flash density maxima occurred within 60 km of the center. The four moderate or strong hurricanes had an inner core maximum of less than 30 flashes (100 km)$^{-2}$ day^{-1}, whereas all marginal hurricanes other than Charley had eyewall maxima exceeding 100 flashes (100 km)$^{-2}$ day^{-1}. Thus, although no clear relationship occurred between average lightning frequency and average storm intensity over 300 km (Fig. 2), the ground flash density maximum in the core was generally larger in marginal than in strong hurricanes.

In the study of Hurricane Andrew, Molinari et al. (1994) defined the term ''eyewall flashes'' as those occurring within 40 km of the storm center. The five marginal hurricanes in this study are likely to have only partial eyewalls and no visible eye, making it difficult to identify flashes as being associated with an eyewall. As a result, the evolution of eyewall flashes will be examined (section 4d) only for the four moderate-to-strong storms (Hurricanes Elena, Gloria, Hugo, and Bob 1991).

The second and third distinct features in Fig. 3 are the low flash density extending 80–100 km outside the inner flash density maximum, and an outer maximum in flash density at radii between 210 km and 290 km.

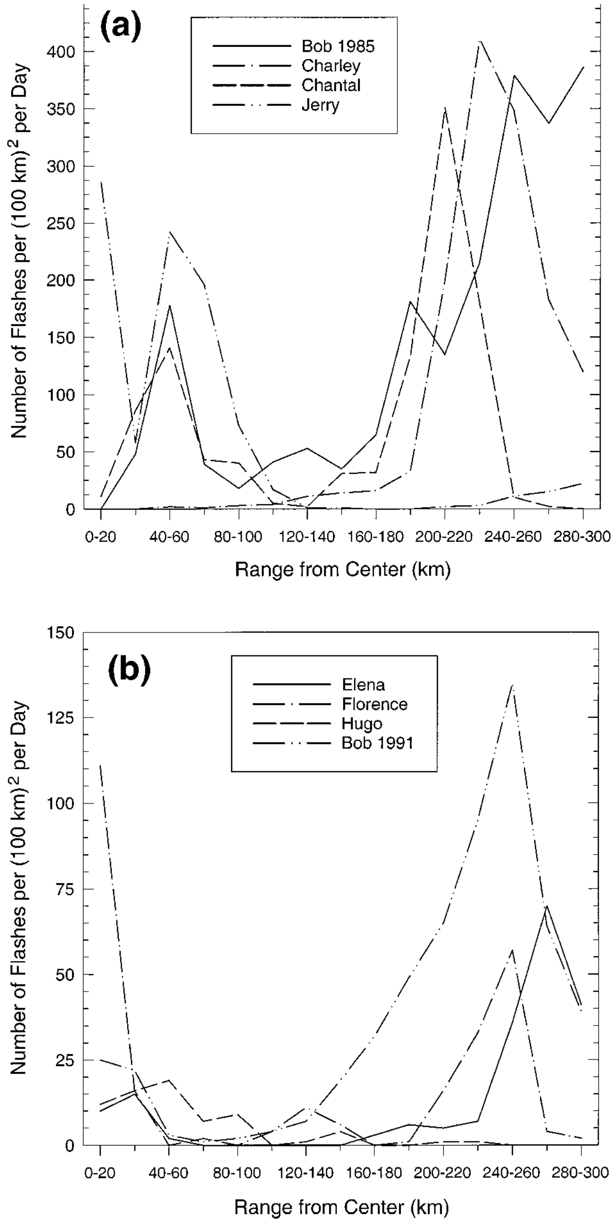

FIG. 3. Radial distribution of ground flash density (number per 10 000 km^2 day^{-1}) during hurricane stage only. (a) Storms with maximum flash density greater than 250 flashes (100 km)$^{-2}$ day^{-1}. (b) Storms with maximum flash density less than 150 flashes (100 km)$^{-2}$ day^{-1}.

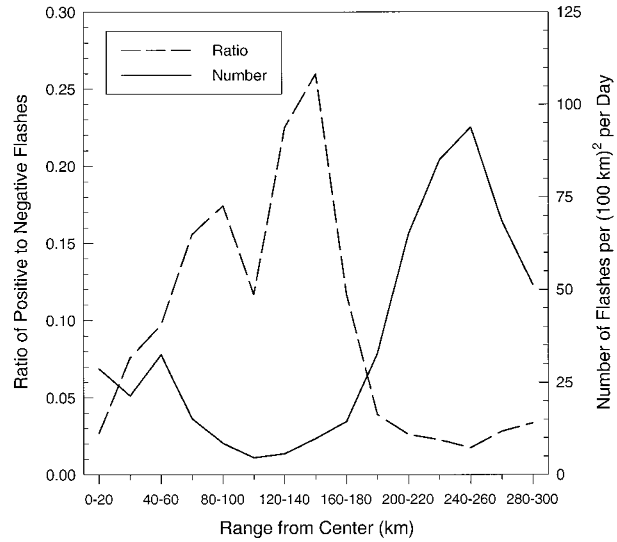

FIG. 4. Radial variation of the ratio of positive to negative flashes (dashed, left axis) and flash density of all flashes (number per 100 km × 100 km box day^{-1}; solid), computed by summing all flashes for the nine hurricanes listed in Table 1.

Hurricanes Jerry and Hugo were exceptions to this radial variation of flash density, in that Jerry contained two inner maxima, and both storms had few outer flashes. These storms were observed for only 12 and 16 h, respectively, and both were over land for half the observing period, so it is possible that the distributions are not characteristic of the storms during their entire life cycle.

Figure 4 shows the radial variation during hurricane stage of the ratio of positive to negative flashes, superimposed on the radial variation of total flash density summed over the nine storms. Because positive flashes were generally infrequent, the radial variation of this quantity from storm to storm was highly erratic; the ratio was not determined at each radial interval for each storm and then averaged. Rather, all flashes for all storms were summed before determining the ratio, and the result in Fig. 4 is most heavily influenced by the storms with the most flashes.

Figure 4 shows that the percentage of positive flashes was largest in a region extending from outside the inner flash density maximum to the radius at which outer rainbands typically originated. In this region, which represents a well-defined minimum in overall cloud-to-ground lightning activity, the ratio of positive to negative flashes exceeds 25%. Holle et al. (1994) showed that the trailing stratiform region of a mesoscale convective system (MCS) had a much higher frequency of positive flashes than in other parts of the MCS, but such flashes were still less than 50% of the total. Overall in the MCS, when convective regions were included as well, positive flashes were only 4% of the total, similar to what is seen in this study. As a result, the region of the hurricane from outside the eyewall to the radius of outer rainband initiation has similarities to the trailing stratiform region of MCSs. Holle et al. (1994) showed one major difference in the overland MCS they studied: a flash rate of 1200–7200 (100 km)$^{-2}$ day^{-1}, about an order of magnitude larger than in the hurricanes in this study.

The third major feature of the radial distribution of flash density is the outer maximum. This feature occurred more than 200 km from the center in every storm except sparsely sampled Hurricane Hugo. With the exceptions of undersampled Hurricanes Jerry, Hugo, and Florence, every hurricane had a stronger outer maximum in flash density than in the eyewall region. The radius of maximum flash density indicates that the vast majority of the lightning must be associated with outer rainbands. By implication, the dramatic differences in flash frequency from storm to storm must relate, at least in part, to the presence or absence of outer rainbands. Because annular area increases with radius, the predominance of outer radius flashes is even more striking in terms of actual numbers of flashes. For the nine hurricanes combined, fewer than 1% of flashes at hurricane intensity occurred within 40 km of the center, and only 3.4% occurred within 80 km.

The radial variation of ground flash density described above provides a confirmation of the distribution found in Hurricane Andrew, which was identical in shape to the storms in this study, but reduced in radial scale.

Figures 5a,b show plots of all negative and positive ground flashes with respect to hourly storm center positions during hurricane stage only. The inner core and outer ground flash maxima, and the intermediate flash minimum, show clearly. Positive flashes are often located just radially outward from clusters of negative flashes, particularly in the low flash density inner band region.

A dramatic azimuthal variation of lightning activity is apparent in Fig. 5. Because most storms had the nearest land either to the north or the west (see Fig. 1), the quadrant nearest to the NLDN on average was the northwest quadrant, where flash counts are minimal. This suggests that distance from the NLDN did not play the primary role in determining the azimuthal variation, and the variation shown is likely to be a reasonable representation of what occurred in reality. Nevertheless, it is open to question whether such a distribution would be common in other locations, or even for other hurricanes in the same locations. In Hurricane Andrew, for instance, the highest flash density occurred north and northeast of the center (Molinari et al. 1994). The azimuthal distribution of lightning is likely to vary with the direction of vertical wind shear, the presence of isolated upper-tropospheric phenomena interacting with the hurricane, the distribution of land and ocean, and the variation between the storm motion and the basic current. As a result, general conclusions are difficult to make. Possibly the most significant characteristic of Fig. 5 is simply that the distance dependence of lightning detection in the NLDN apparently played no substantial role in the results of this paper.

Comparisons will be made with the prehurricane stages of three storms. The definition of "hurricane" intensity was made long before the availability of the sophisticated instruments of recent years and might appear to be somewhat arbitrary. Shapiro and Willoughby (1982) have shown, however, that an eyelike structure tends to develop in response to diabatic heating in a balanced model when the mean tangential velocity reaches about 35 m s^{-1}. This value is very close to the 34 m s^{-1} definition of hurricane strength. In practice, a well-defined eye and eyewall are much more likely to occur at hurricane intensity than before (P. Black 1996, personal communication). The above arguments suggest that the separation of tropical cyclones into hurricane and prehurricane stages is meaningful.

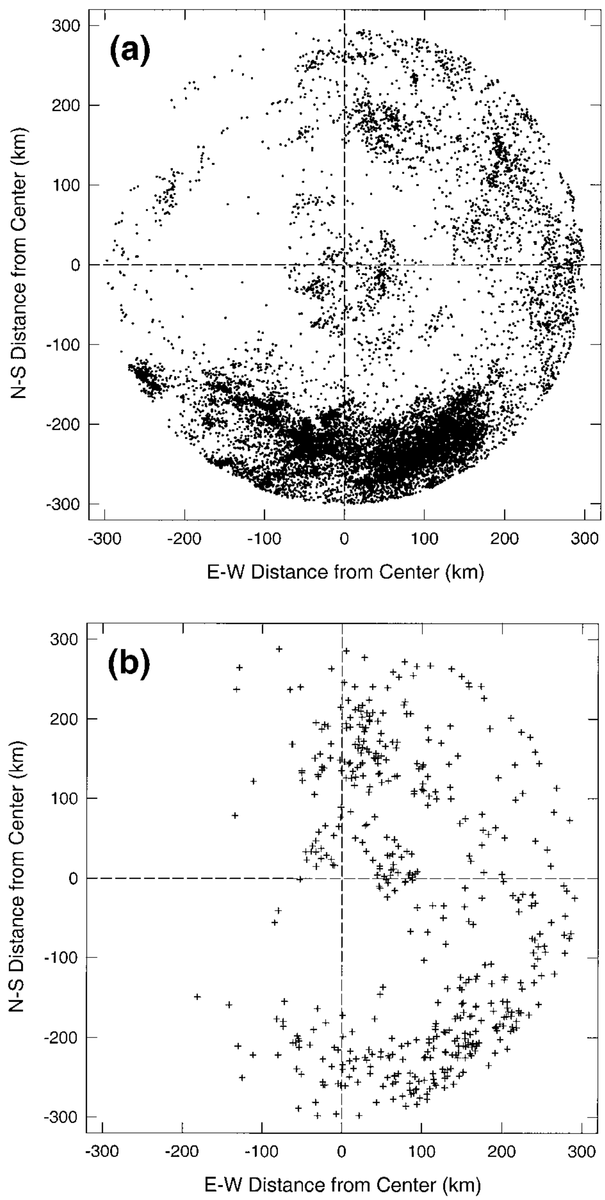

FIG. 5. Plot of the locations of all negative ground flashes (a) and positive ground flashes (b) during hurricane stage in the nine storms listed in Table 1, composited with respect to the hourly center position of each hurricane.

Figure 6 shows the pre-hurricane radial variation of ground flash density for the three available storms. None of the three had the characteristic radial distribution seen at hurricane stage. Tropical Depression/Storm Bob

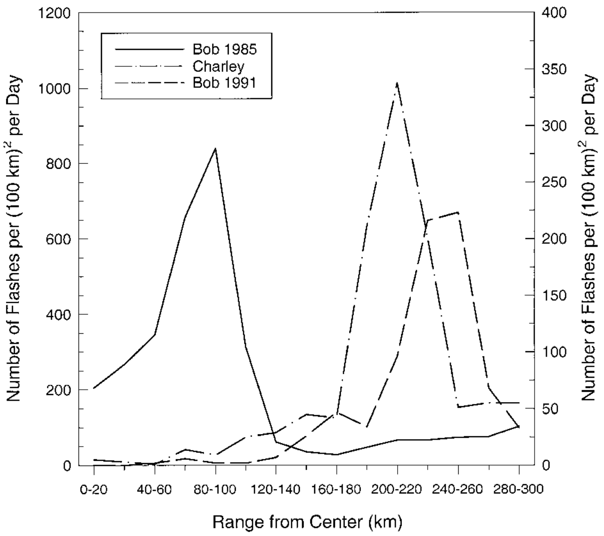

FIG. 6. As in Fig. 3 but for the prehurricane stages of three hurricanes. The scale for Bob (1985) is on the left axis; the scale for the other two storms is on the right axis.

(1985) had a strong maximum at the 90-km radius, where hurricane-strength disturbances have few flashes (Fig. 3), and had no distinct outer maximum. Tropical Storms Charley (1986) and Bob (1991) had only outer maxima. None of the three showed evidence of a flash density maximum near the storm core. Once they reached hurricane strength, two of the three (the exception being subtropical storm Charley) developed the inner core maximum, the sharp minimum outside of the core, and the strong outer maximum characteristic of hurricanes.

c. Time variation

Figures 7a–d show the evolution of flash frequency within 300 km of the center for storms with more than 2500 total flashes, superimposed on the minimum central pressure of the storm. For all storms the flash rate varied considerably in time. These changes largely mirrored the activity level in outer rainbands.

The time variation diagrams are remarkable more for their lack of coherence than anything else. No discernible diurnal variation in lightning frequency occurred in the storms. Two of the storms had one large outburst of lightning (Bob 1985, and Elena), while the other two had many fluctuations with no apparent periodicity. No systematic relationship existed between instantaneous flash frequency and storm intensity or sign of intensity change on this 300-km scale, with one exception: a relative maximum in lightning frequency occurred during hurricane stage in the four storms just prior to maximum intensity.

When all nine storms are considered, along with Hurricane Andrew (Fig. 4 of Molinari et al. 1994), the time variation of flash frequency over 300 km displayed one other common behavior: a strong rise in flash rate in the hours prior to landfall in four of the five marginal hurricanes (Charley, Chantal, Jerry, and Bob 1985), and no significant change prior to landfall in moderate-to-severe hurricanes (Elena, Gloria, Hugo, Andrew, and Bob 1991). The reasons for this behavior are unclear.

d. Relationship of eyewall flashes to structure and intensity change

As noted earlier, flashes occurring within the 40-km radius (‘‘eyewall flashes’’) will be examined only for the four relatively strong hurricanes in Table 1. Molinari et al. (1994) showed that most eyewall flashes in Hurricane Andrew occurred on the inner edge of the eyewall as seen from satellite. Aircraft reconnaissance observations indicate that during the times of lightning data collection, Hurricanes Elena, Gloria, Hugo, and Bob (1991) had eyewalls that were sometimes completely closed, sometimes open to one side, but that were always definable, with diameters of the order of 40 km or less.

Figure 8 shows the frequency of eyewall flashes in three hurricanes, superimposed upon the trace of minimum sea level pressure in the storms. Hurricane Gloria had no flashes within 40 km of the center during the time it was within range of the NLDN. It is apparent that eyewall lightning is relatively rare, occurring in 7 of 74 hours in Hurricane Elena, 3 of 16 hours in Hurricane Hugo, 4 of 71 hours in Hurricane Bob (1991), and 0 of 33 hours in Hurricane Gloria. Even neglecting 1-h gaps, eyewall lightning never occurred for as long as 6 h in these storms. In three of the hurricanes an outbreak occurred within 6 h of maximum intensity. An eyewall outbreak occurred in Hurricane Elena just before a period of rapid deepening began. In this section the physical significance of these eyewall lightning outbreaks will be examined.

It was suggested by Molinari et al. (1994) that eyewall cycles may be accompanied by outbreaks of eyewall lightning. In such cycles, a second eyewall develops outside the existing one, then often contracts and replaces the original eyewall. These cycles are typically identified by dual maxima in wind speed (Willoughby et al. 1982). The eyewall replacement process can bring about a weakening of the inner wind maximum and filling of the storm, followed by renewed deepening as the second eyewall becomes the primary one (Willoughby et al. 1982; Willoughby 1990). Such cycles are most common in moderate or intense hurricanes. Willoughby (1996, personal communication) has noted that eyewall cycles also can begin as a storm reaches its maximum potential intensity for the given sea surface temperature. Under such circumstances the development of an outer eyewall can produce a dramatic reversal from deepening to filling of the hurricane. The large intensity changes associated with eyewall cycles makes knowledge of their existence quite useful to hurricane forecasters.

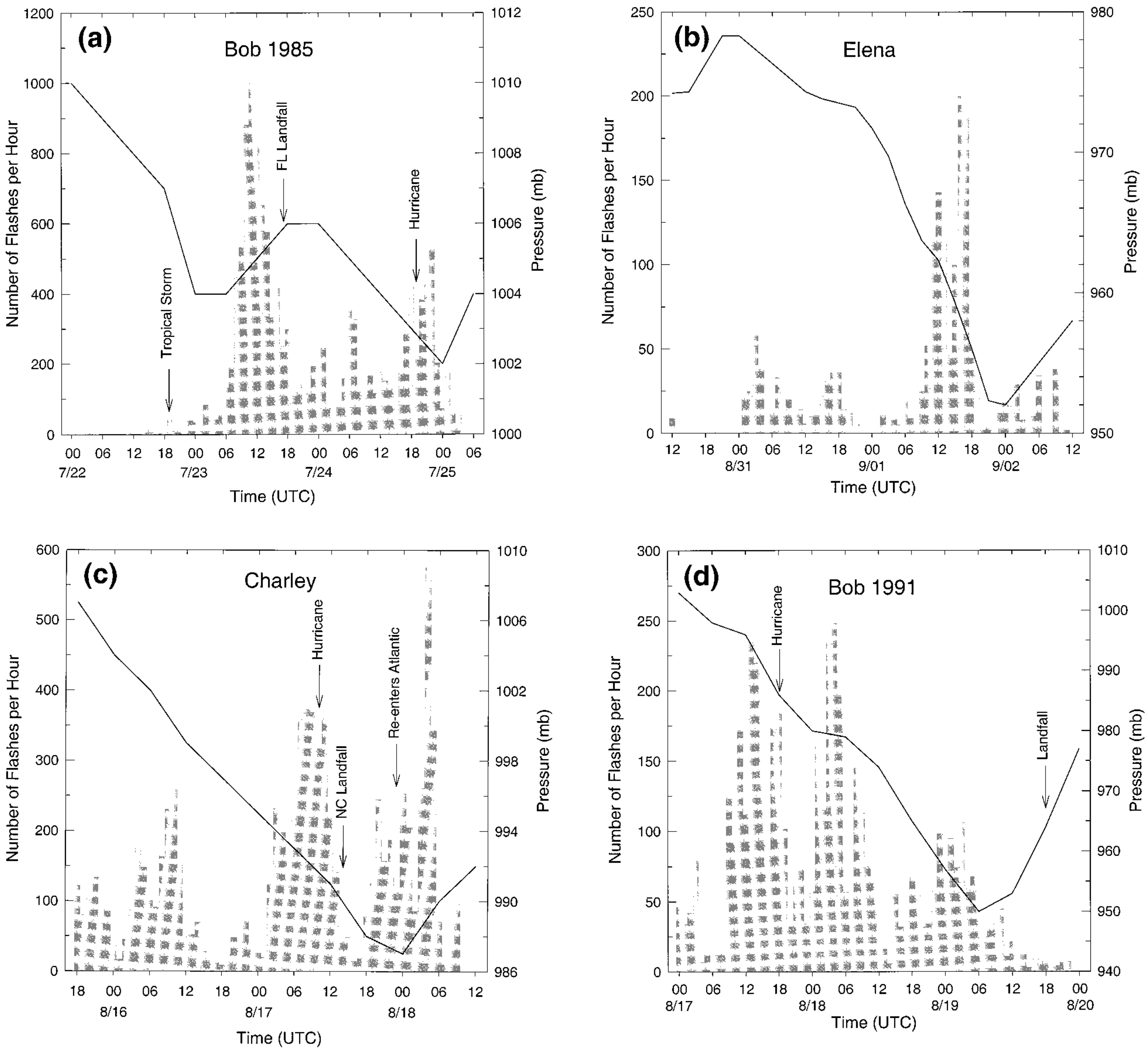

FIG. 7. Time variation of the number of cloud-to-ground flashes within 300 km of the center, superimposed on a 6-hourly trace of minimum central pressure (3-hourly for Hurricane Elena), for each storm that was observed for more than 48 h: (a) Hurricane Bob (1985), (b) Hurricane Elena (1985), (c) Hurricane Charley (1986), and (d) Hurricane Bob (1991). The vertical axis scale has been adjusted for each storm.

Eyewall cycles are usually hidden on visible and infrared satellite images by the thick cirrus overcast, and must be identified by reconnaissance aircraft. If lightning data could identify such cycles, it would provide a valuable additional tool.

1) HURRICANE ELENA

The evolution of Hurricane Elena on the synoptic scale has been studied by Molinari and Vollaro (1989, 1990) and Molinari et al. (1995). A series of water vapor channel images over the life cycle of the storm is given by Velden (1987). The radial variation of precipitation in Hurricane Elena within 80 km of the core was examined by Burpee and Black (1989) for the period 1430 UTC 1 September to 0130 UTC 2 September. Burpee and Black found that precipitation had characteristics of stratiform rain from outside the eyewall (which was at r = 35 km) to the 80-km edge of their region, but was much more convective within the eyewall, particularly at about 1700 UTC and 2330 UTC 1 September. These findings are consistent with the sharp dropoff of flash density outside the 40-km radius in Hurricane Elena shown in Fig. 3b. Figure 8a shows eyewall lightning associated with the 1700 UTC convective precipitation maximum, but not with that at 2300 UTC.

Of the storms in the current study, only for Hurricane Elena have eyewall cycles been formally analyzed, by

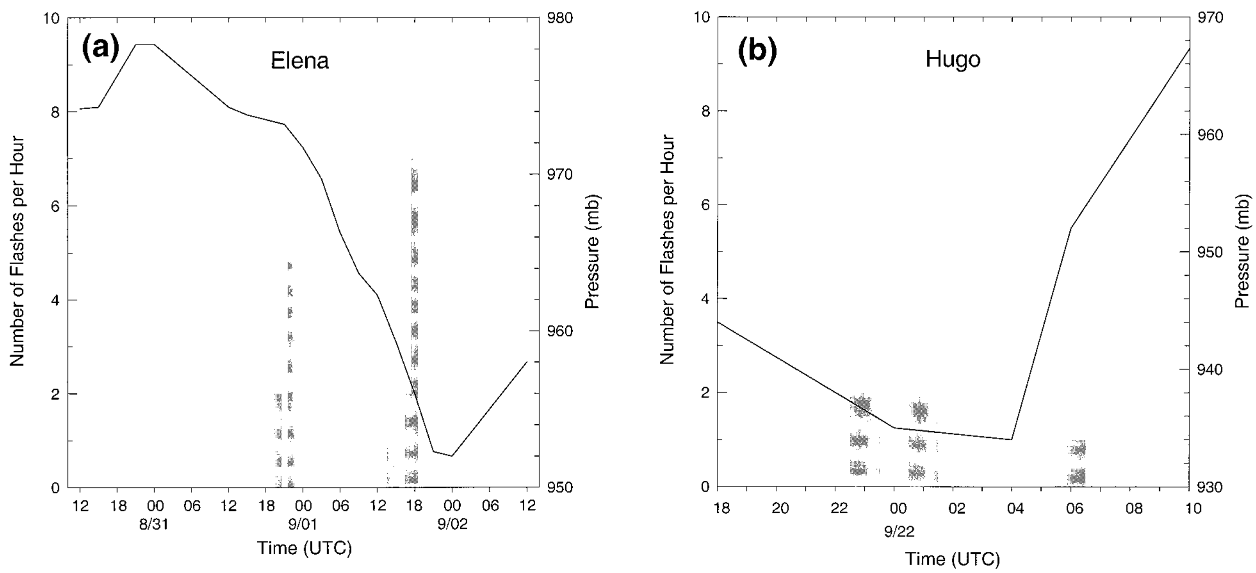

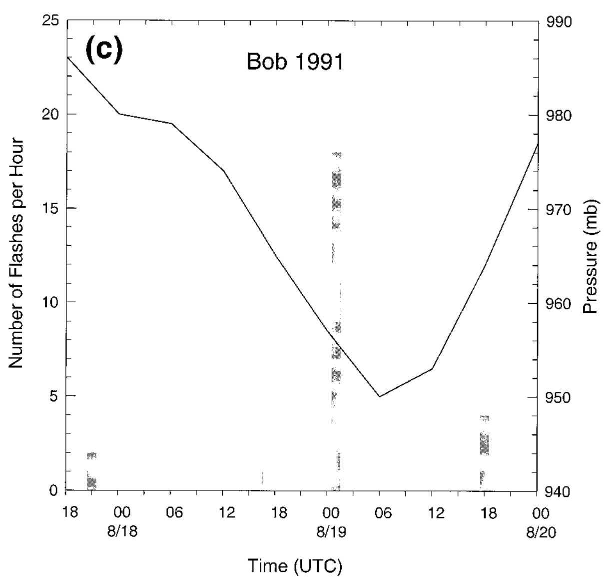

FIG. 8. As in Fig. 7 but for flashes within 40 km of the center in (a) Hurricane Elena, (b) Hurricane Hugo, and (c) Hurricane Bob (1991). Also shown are 6-hourly traces of minimum central pressure in the storms (3-hourly for Elena), supplemented by the pressure at landfall (0400 UTC 22 September 1989) for Hurricane Hugo.

Willoughby (1990). He identified three eyewall cycles in the storm [see also Figs. 8 and 9 of Molinari and Vollaro (1990) and Fig. 1 of Samsury and Zipser (1995)], two of which occurred when the storm was within range of the NLDN. The first of these, as defined by fluctuations in the lower-tropospheric wind field by Willoughby (1990), occurred between approximately 0600 UTC and 2200 UTC 31 August, as the outer eyewall moved from about the 120-km radius to the 20-km radius. The second occurred between 0800 UTC and 1800 UTC 1 September 1985, as an outer eyewall moved from the 30-km radius to inside the 20-km radius.

Figure 8a shows that eyewall lightning in Hurricane Elena occurred each time as the secondary eyewall became the primary eyewall in the hurricane core. The first of these led to a period of rapid deepening as the new eyewall reached the 20-km radius (see Molinari and Vollaro 1990). Infrared satellite images (not shown) indicate that an eyewall open to the west became fully closed during this period, not unlike what occurred in Hurricane Andrew over the Gulf of Mexico (Molinari et al. 1994, plate 2). The second eyewall cycle occurred just before maximum intensity and was followed by a reversal of deepening. In both cases the development of an eyewall cycle resulted in major changes in storm intensity. It is notable that both events were accompanied by outbreaks of eyewall lightning, and that eyewall lightning occurred only when eyewall cycles were taking place.

2) HURRICANES HUGO, BOB (1991), AND GLORIA

Figure 8b shows that Hurricane Hugo had a small outbreak of eyewall lightning 3–5 h before landfall, during the final part of its rapid deepening. Samsury and Orville (1994) show that these flashes did indeed occur within the eyewall. The eyewall flashes in this case do not appear to represent an eyewall cycle [see Fig. 4 of Samsury and Orville (1994)], but they gave early warning to the fact that the storm was continuing to deepen as it approached the coast.

Figure 8c shows that one major outbreak of eyewall lightning occurred in Hurricane Bob (1991), at 0100 UTC 19 August. Aircraft reconnaisance pilots reported the development of a secondary wind maximum about 100 km from the hurricane center just before 0300 UTC 19 August; the hurricane reached its maximum intensity as measured by central pressure at 0400 UTC (these intermediate values do not show on the 6-hourly best-track data in Fig. 8c); and the storm began to change its direction and speed of motion (from northward at 9 m s^{-1} to north-northeastward at 13 m s^{-1}) at 0400 UTC 19 August. As a result, an outbreak of eyewall lightning once again appears to indicate imminent change in the intensity and structure of the hurricane.

Hurricane Gloria had no eyewall flashes. During the 33 h it was within range of the NLDN at hurricane strength, its pressure was almost unvarying, remaining between 942 and 946 mb until it filled at landfall. This provides a null case for comparison with the others; just as an outbreak of eyewall lightning appeared to signal imminent change in Hurricanes Elena, Hugo, and Bob (1991), the absence of eyewall lightning was associated with a lack of meaningful change in Hurricane Gloria.

5. Discussion

Each storm in this study had unique characteristics with regard to its intensity, variation of underlying ocean temperature, dynamical interactions with its environment, and frequency and nature of encounters with land surfaces. Under these circumstances it is rather remarkable that such a regular radial distribution of lightning occurred at hurricane intensity. The results support the division of the hurricane by Molinari et al. (1994) into three zones of distinct electrical characteristics, and thus presumably of distinct convective character: the inner core, which contains a weak maximum in flash density; a region with a well-defined minimum in flash density extending 80–100 km outside this maximum; and the outer band region, which contains a strong maximum in flash density outside the 200-km radius.

The three available prehurricane datasets showed neither an inner core flash maximum nor a sharp minimum outside the core. The lack of these features suggests that development of the eyewall plays a prominent role in shaping the convective structure of the hurricane within about 100 km of the center.

a. Inner core region

The moderate-to-strong hurricanes in this study contained inner core flash density maxima below 30 flashes (100 km)$^{-2}$ day^{-1}, whereas four of the five marginal hurricanes had maxima in excess of 100 (100 km)$^{-2}$ day^{-1}. Although marginal hurricanes are unlikely to have a fully formed eyewall in all quadrants, the results suggest that whatever core convection occurs in weaker storms is more electrified. Once a strong hurricane developed, lightning in the vicinity of the eyewall was episodic, occurring in only 7% of the hourly periods of the four relatively strong hurricanes in this study. In these storms, eyewall lightning never occurred for more than 5 h, even when the storm deepened for a much longer period.

The reasons for the rarity of ground flashes in the vicinity of the eyewall have been addressed by Black and Hallett (1986; 1997), Black et al. (1993), and Molinari et al. (1994). Black and Hallett (1986) noted the absence of supercooled water in the eyewall, which makes significant charge separation unlikely by current theories of noninductive charge transfer between ice particles in the presence of liquid water (Saunders 1993). Black and Hallett (1986) attributed the lack of supercooled water to the efficient seeding of eyewall clouds by ice in the rapidly rotating storm core, and to the relative lack of strong updrafts. Recently Black et al. (1996) have shown via vertically pointing Doppler radar in several storms that more than 70% of eyewall updrafts and downdrafts have a magnitude less than 2 m s^{-1} (averaged horizontally over 750 m). This is consistent with the results of Szoke et al. (1986) and Jorgensen et al. (1985) that eyewall updrafts do not differ dramatically in magnitude from those of oceanic convective clouds during the GATE experiment. Molinari et al. (1994) likened the eyewall to the weakly electrified oceanic monsoon convection found in subtropical Australia by Rutledge et al. (1992) and Williams et al. (1992). In both situations the cloud is deep, but the reflectivity maximum is typically below the mixed phase region (Marks and Houze 1987), reflectivity decreases rapidly upward above the melting level (Szoke et al. 1986), and most updrafts are in the range of 1–10 m s^{-1} (Williams et al. 1992; Black et al. 1996). Unlike the monsoon clouds, however, the eyewall can tilt outward at a 45° angle (Marks and Houze 1987), and its updrafts are considerably wider than in ordinary tropical convection (Jorgensen et al. 1985). In addition, the eyewall represents a region of extremely high surface θ_e, yet low flash rate, a characteristic not seen in more ordinary convection (Williams 1995). These characteristics arise from the strong dynamical control of eyewall circulation in the rapidly rotating but nearly balanced core (Willoughby 1988; Shapiro and Montgomery 1993). By implication, the episodic occurrence of eyewall lightning may indicate an outbreak of buoyancy-driven updrafts and temporary disruption of such balance. Although the hurricane eyewall has some characteristics of tropical oceanic convection, it represents a unique atmospheric phenomenon with its own dynamical, microphysical (Black and Hallett 1986), and electrical organization.

b. Flash minimum outside the inner core

Ground flash density in hurricanes drops off sharply in an approximately 100-km wide annular region outside the eyewall and radially inside the outer bands. Every storm other than Hurricane Bob (1985) contained a relatively wide region of virtually no flashes (Fig. 3). When all ground flashes in all storms are added (Fig. 4), the minimum flash density, 5 flashes $(100\ \mathrm{km})^{-2}\ \mathrm{day}^{-1}$, occurs 100–120 km from the center. In general, this region lies underneath the dense cirrus overcast common to hurricanes. Molinari et al. (1994) called it the ''inner band region,'' because banded precipitation still occurs despite the lack of ground flashes.

Inner bands frequently contain a bright band on radar (Marks and Houze 1987; Szoke et al. 1986; Jorgenson 1984) associated with the growth and fallout of frozen hydrometeors that have been ejected from the eyewall (Marks and Houze 1987; Black and Hallett 1986; Barnes et al. 1983; Lord et al. 1984; Houze et al. 1992). The brightband regions often contain lower-tropospheric downdrafts and suppressed convection that can extend more than 100 km from the center (Marks and Houze 1987). It is thus not surprising that within 100 km of the center, even when the eyewall is included, stratiform rain covers 10 times the area of convective rain, and accounts for more than half the precipitation (Marks 1985; Marks et al. 1992).

Data from this study supply further evidence of the nature of the inner band region. Overall ground flash activity is substantially lower than anywhere else in the hurricane, consistent with the lack of observed supercooled water (Black and Hallett 1986; Houze et al. 1992). In addition, the fraction of positive ground flashes is significantly elevated in the region where overall flash rate is a minimum. This suggests that the inner band region resembles the trailing stratiform region of mesoscale convective systems. In hurricanes, the dense cirrus overcast created by debris ejected from the eyewall appears to act like the anvil region of an MCS.

c. Outer band region

In this study, every storm observed for longer than 16 h had a large flash density maximum in outer bands. As in the Hurricane Andrew study, the outer bands were often observed to form outside the storm core and to propagate with respect to both the ground and the storm center. Their existence outside the central dense overcast is consistent with the numerical modeling results of Lord et al. (1984). Some of these bands last for several hours (see plate 1 of Molinari et al. 1994).

Willoughby et al. (1984) proposed that outside the ''principal band,'' which typically occurs between 75 and 125 km from the center, environmental air flows around the storm. Outer bands, with their radius of maximum flash density about 250 km from the storm center (Figs. 3 and 4) clearly fall into this region of environmental air. In support of this, the ratio of positive to negative flashes in outer rainbands closely resembles that of a background state in the same region in the absence of hurricanes (Molinari et al. 1994). The environmental air is convectively unstable, as shown by Jordan's (1958) mean West Indies sounding during hurricane season [see the discussion associated with Fig. 2.2.10 by Williams (1995)], and by monthly mean soundings of Gulf of Mexico coastal stations (not shown). The typically unstable soundings in the hurricane environment might make it more likely that sufficiently large updrafts needed for charge separation will occur in outer bands. This cannot, however, be a complete explanation. Tropical and subtropical oceanic convection often has convective available potential energy values as large as over land (Zipser and LeMone 1980), but it does not realize as high a fraction of the pseudoadiabatic ascent rate (Jorgenson and LeMone 1989) and contains much smaller ground flash rates than over land (see, e.g., Lucas and Orville 1996). The reason for the large flash density in outer bands remains somewhat uncertain.

d. Predictive value of eyewall flashes

In Hurricane Andrew (Molinari et al. 1994), eyewall flashes were episodic and occurred during or just before periods of intensification. The episodic nature of eyewall flashes was true of the four strong hurricanes in this study as well, but such outbreaks often occurred within hours of the end of a deepening period. This behavior suggests that eyewall cycles were occurring. For the one storm in which eyewall cycle information was available (Hurricane Elena), both eyewall cycles were accompanied by outbreaks of lightning. Because such phenomena can only rarely be seen on satellite, yet often produce large intensity changes in the storm, the identification of such cycles is a major potential benefit of lightning data. Although the NLDN can only track such changes when the storms are within approximately 400 km of land, this circumstance is exactly when such knowledge would be of greatest value to forecasters and civil defense interests.

It is proposed that an outbreak of lightning in the core of a weakening, steady, or slowly deepening hurricane might indicate it is about to rapidly intensify. This occurred in Hurricanes Elena (first outbreak in Fig. 8a) and Andrew [first outbreak in Fig. 5 of Molinari et al. (1994)]. In contrast, an outbreak of lightning in the core of a hurricane that has been deepening for some time may indicate the imminent end, or even reversal, of the intensification. This occurred in the second event in Hurricane Elena (Fig. 8a) and the event in Hurricane Bob of 1991 (Fig. 8c). Finally, the lack of inner core flashes may indicate little change in the hurricane, as shown by the lack of any eyewall flashes while Hurricane Gloria was nearly steady. Although only a few cases have been examined, it appears that knowledge of eyewall ground flashes in mature tropical cyclones might prove to be useful for intensity prediction of such storms.

Acknowledgments. We are indebted to Global Atmospherics, Inc. for providing the revised site corrections used to process the NLDN data. We benefitted from comments on the manuscript by Drs. Ed Zipser and Earle Williams. We thank Gretchen Heller for helping to generate the data for Hurricane Florence. Paul Bogner (now of the University of Hawaii) examined the accuracy of the NLDN locations for the revised site corrections as part of an undergraduate independent study project. This work was supported by National Science Foundation Grant ATM9423229.

REFERENCES

Barnes, G. M., E. J. Zipser, D. Jorgensen, and F. Marks Jr., 1983: Mesoscale and convective structure of a hurricane rainband. *J. Atmos. Sci.,* **40,** 2125–2137.

Black, M. L., R. W. Burpee, and F. D. Marks Jr., 1996: Vertical motion characteristics of tropical cyclones determined with airborne Doppler radial velocities. *J. Atmos. Sci.,* **53,** 1887–1909.

Black, R. A., and J. Hallett, 1986: Observations of the distribution of ice in hurricanes. *J. Atmos. Sci.,* **43,** 802–822.

——, and ——, 1999: The electrification of the hurricane. *J. Atmos. Sci.,* in press.

——, ——, and C. P. R. Saunders, 1993: Aircraft studies of precipitation and electrification in hurricanes. Preprints, *17th Conf. on Severe Local Storms,* St. Louis, MO, Amer. Meteor. Soc., J20–J25.

Brook, M., M. Nakano, P. Krehbiel, and T. Takeuti, 1982: The electrical structure of the Hokuriko winter thunderstorms. *J. Geophys. Res.,* **87,** 1207–1215.

Burpee, R. W., and M. L. Black, 1989: Temporal and spatial variations of rainfall near the centers of two tropical cyclones. *Mon. Wea. Rev.,* **117,** 2204–2218.

Cummins, K. L., W. L. Hiscox, A. E. Pifer, and M. W. Maier, 1992: Performance analysis of the U.S. National Lightning Detection Network. *Proc. Ninth Int. Conf. on Atmospheric Electricity*, St. Petersburg, Russia, International Commission on Atmospheric Electricity, 914–919.

——, M. J. Murphy, E. A. Bardo, W. L. Hiscox, R. B. Pyle, and A. E. Pifer, 1998: A combined TOA/MDF technology upgrade of the U.S. National Lightning Detection Network. *J. Geophys. Res.,* **103,** 9035–9044.

Engholm, C. D., E. R. Williams, and R. M. Dole, 1990: Meteorological and electrical conditions associated with positive cloud-to-ground lightning. *Mon. Wea. Rev.,* **118,** 470–487.

Hiscox, W. L., E. P. Krider, A. E. Pifer, and M. A. Uman, 1984: A systematic method for identifying and correcting site errors in a network of magnetic direction finders. *Int. Aerospace and Ground Conf. on Lightning and Static Electricity,* Williamsburg, VA, NASA, FAA, and U.S. Departments of Navy, Army, and Air Force, 33–38.

Holle, R. L., and R. E. López, 1993: Overview of real-time lightning detection systems and their meteorological uses. NOAA Tech. Memo. ERL NSSL-102, 68 pp. [Available from National Technical Information Service, Sills Building, 5285 Port Royal Road, Springfield, VA 22161.]

——, A. I. Watson, R. E. López, D. R. MacGorman, R. Ortiz, and W. D. Otto, 1994: The life cycle of lightning and severe weather in a 3–4 June 1985 PRE-STORM mesoscale convective system. *Mon. Wea. Rev.,* **122,** 1798–1808.

Horner, F., 1954: The accuracy of the location of sources of atmospherics by radio direction finding. *Proc. IEEE,* **101,** 383–390.

Houze, R. A., Jr., F. D. Marks Jr., and R. A. Black, 1992: Dual-aircraft investigation of the inner core of Hurricane Norbert. Part II: Mesoscale distribution of ice particles. *J. Atmos. Sci.,* **49,** 943–962.

Idone, V. P., D. A. Davis, P. K. Moore, Y. Wang, R. W. Henderson, M. Ries, and P. F. Jamason, 1998a: Performance evaluation of the National Lightning Detection Network in eastern New York. Part I: Detection efficiency. *J. Geophys. Res.,* in press.

——, ——, ——, ——, ——, ——, and ——, 1998b: Performance evaluation of the National Lightning Detection Network in eastern New York. Part II: Location accuracy. *J. Geophys. Res.,* in press.

Jordan, C. L., 1958: Mean soundings for the West Indies area. *J. Meteor.,* **15,** 91–97.

Jorgensen, D. P., 1984: Mesoscale and convective scale characteristics of mature hurricanes. Part II: Inner core structure of Hurricane Allen (1980). *J. Atmos. Sci.,* **41,** 1287–1311.

——, and M. A. LeMone, 1989: Vertical velocity characteristics of oceanic convection. *J. Atmos. Sci.,* **46,** 621–640.

——, E. J. Zipser, and M. A. LeMone, 1985: Vertical motions in intense hurricanes. *J. Atmos. Sci.,* **42,** 839–856.

Knight, P., 1967: Re-radiation from masts and similar obstacles at radio frequencies. *Proc. IEEE,* **96,** 321–332.

Krishnamurti, T. N., and H. N. Bhalme, 1976: Oscillations of a monsoon system. Part I: Observational aspects. *J. Atmos. Sci.,* **33,** 1937–1954.

Lascody, R. A., 1992: A different look at Hurricane Andrew—Lightning around the eyewall. *Natl. Wea. Dig.,* **17,** 39–40.

Lord, S. J., H. E. Willoughby, and J. M. Piotrowicz, 1984: Role of a parameterized ice-phase microphysics in an axisymmetric, nonhydrostatic tropical cyclone model. *J. Atmos. Sci.,* **41,** 2836–2848.

Lucas, C., and R. E. Orville, 1996: TOGA COARE: Oceanic lightning. *Mon. Wea. Rev.,* **124,** 2077–2082.

Lyons, W. A., and C. S. Keen, 1994: Observations of lightning in convective supercells within tropical storms and hurricanes. *Mon. Wea. Rev.,* **122,** 1897–1916.

MacGorman, D. R., and D. W. Burgess, 1994: Positive cloud-to-ground lightning in tornadic storms and hailstorms. *Mon. Wea. Rev.,* **122,** 1671–1697.

Maier, M. W., 1991: Preliminary evaluation of NLDN performance at Cape Canaveral during August 1990. CSR Instrumentation Systems Evaluation Test Rep. CDRL 137A2, 24 pp. [Available from Computer Sciences, Raytheon, P.O. Box 4127, Patrick Air Force Base, FL 32925.]

Marks, F. D., Jr., 1985: Evolution of the structure of precipitation in Hurricane Allen (1980). *Mon. Wea. Rev.,* **113,** 909–930.

——, and R. A. Houze Jr., 1987: Inner core structure of Hurricane Alicia from airborne Doppler radar observations. *J. Atmos. Sci.,* **44,** 1296–1317.

——, ——, and J. F. Gamache, 1992: Dual-aircraft investigation of the inner core of Hurricane Norbert. Part I: Kinematic structure. *J. Atmos. Sci.,* **49,** 919–942.

Molinari, J., and D. Vollaro, 1989: External influences on hurricane intensity. Part I: Outflow layer eddy angular momentum fluxes. *J. Atmos. Sci.,* **46,** 1093–1105.

——, and ——, 1990. External influences on hurricane intensity. Part II: Vertical structure and response of the hurricane vortex. *J. Atmos. Sci.,* **47,** 1902–1918.

——, P. K. Moore, V. P. Idone, R. W. Henderson, and A. B. Saljoughy, 1994: Cloud-to-ground lightning in Hurricane Andrew. *J. Geophys. Res.,* **99,** 16 665–16 676.

——, S. Skubis, and D. Vollaro, 1995: External influences on hurricane intensity. Part III: Potential vorticity structure. *J. Atmos. Sci.,* **52,** 3593–3606.

Orville, R. E., 1991: Calibration of a magnetic direction finding network using measured triggered lightning return stroke peak currents. *J. Geophys. Res.,* **96,** 17 135–17 142.

——, R. W. Henderson, and L. F. Bosart, 1988: Bipole patterns revealed by lightning locations in mesoscale storm systems. *Geophys. Res. Lett.,* **15,** 129–132.

Randell, S. C., S. A. Rutledge, R. D. Farley, and J. H. Helsdon Jr., 1994: A modeling study on the early electrical development of tropical convection: Continental and oceanic (monsoon) storms. *Mon. Wea. Rev.,* **122,** 1852–1877.

Rutledge, S. A., and D. R. MacGorman, 1988: Cloud-to-ground lightning activity in the 10–11 June 1985 mesoscale convective system observed during the Oklahoma–Kansas PRE-STORM project. *Mon. Wea. Rev.,* **116,** 1393–1408.

——, and W. A. Petersen, 1994: Vertical radar reflectivity structure and cloud-to-ground lightning in the stratiform region of MCSs: Further evidence for in situ charging in the stratiform region. *Mon. Wea. Rev.,* **122,** 1760–1776.

——, C. Lu, and D. R. MacGorman, 1990: Positive cloud-to-ground lightning in mesoscale convective systems. *J. Atmos. Sci.,* **47,** 2085–2100.

——, E. R. Williams, and T. D. Keenan, 1992: The down under doppler and electricity experiment (DUNDEE): Overview and preliminary results. *Bull. Amer. Meteor. Soc.,* **73,** 3–16.

Samsury, C. E., and R. E. Orville, 1994: Cloud-to-ground lightning in tropical cyclones: A study of Hurricanes Hugo (1989) and Jerry (1989). *Mon. Wea. Rev.,* **122,** 1887–1896.

——, and E. J. Zipser, 1995: Secondary wind maxima in hurricanes: Airflow and relationship to rainbands. *Mon. Wea. Rev.,* **123,** 3502–3517.

Saunders, C. P. R., 1993: A review of thunderstorm electrification processes. *J. Appl. Meteor.,* **32,** 642–655.

Seimon, A., 1993: Anomalous cloud-to-ground lightning in an F5-tornado-producing supercell thunderstorm on 28 August 1990. *Bull. Amer. Meteor. Soc.,* **74,** 189–203.

Shapiro, L. J., and H. E. Willoughby, 1982: The response of balanced hurricanes to local sources of heat and momentum. *J. Atmos. Sci.,* **39,** 378–394.

——, and M. T. Montgomery, 1993: A three-dimensional balance theory for rapidly rotating vortices. *J. Atmos. Sci.,* **50,** 3322–3335.

Stoltzenburg, M., T. C. Marshall, W. D. Rust, and B. F. Smull, 1994: Horizontal distribution of electrical and meteorological conditions across the stratiform region of a mesoscale convective system. *Mon. Wea. Rev.,* **122,** 1777–1797.

Szoke, E. J., E. J. Zipser, and D. P. Jorgensen, 1986: A radar study of convective cells in mesoscale systems in GATE. Part 1: Vertical profile statistics and comparison with hurricanes. *J. Atmos. Sci.,* **43,** 182–197.

Velden, C. S., 1987: Satellite observations of Hurricane Elena (1985) using the VAS 6.7 micrometer ''water vapor'' channel. *Bull. Amer. Meteor. Soc.,* **68,** 210–215.

Williams, E. R., 1995: Meteorological aspects of thunderstorms. *Handbook of Atmospheric Electrodynamics,* Hans Volland, Ed., CRC, 27–60.

——, S. A. Rutledge, S. G. Geotis, N. Renno, E. Rasmussen, and T. Rickenbach, 1992: A radar and electrical study of tropical ''hot towers.'' *J. Atmos. Sci.,* **49,** 1386–1395.

Willoughby, H. E., 1988: The dynamics of the tropical cyclone core. *Aust. Meteor. Mag.,* **36,** 183–189.

——, 1990: Temporal changes of the primary circulation in tropical cyclones. *J. Atmos. Sci.,* **47,** 242–264.

——, J. A. Clos, and M. G. Shoreibah, 1982: Concentric eyewalls, secondary wind maxima, and the evolution of a hurricane vortex. *J. Atmos. Sci.,* **39,** 395–411.

——, F. D. Marks Jr., and R. J. Feinberg, 1984: Stationary and moving convective bands in hurricanes. *J. Atmos. Sci.,* **41,** 3189–3211.

Yuter, S. E., and R. A. Houze Jr., 1995: Three-dimensional kinematic and microphysical evolution of Florida cumulonimbus. Part I: Spatial distribution of updrafts, downdrafts, and precipitation. *Mon. Wea. Rev.,* **123,** 1921–1940.

——, and ——, 1998: The natural variability of precipitating clouds over the western Pacific warm pool. *Quart. J. Roy. Meteor. Soc.,* **124,** 53–100.

Zipser, E. J., and M. A. LeMone, 1980: Cumulonimbus vertical velocity events in GATE. Part II: Synthesis and model core structure. *J. Atmos. Sci.,* **37,** 2458–2469.

——, and K. R. Lutz, 1994: The vertical profile of radar reflectivity of convective cells: A strong indicator of storm intensity and lightning probability? *Mon. Wea. Rev.,* **122,** 1751–1759.